



Two-Dimensional TiO₂ Ultraviolet Filters for Sunscreens

Cite as

Nano-Micro Lett.

(2025) 17:300

Received: 18 February 2025

Accepted: 13 May 2025

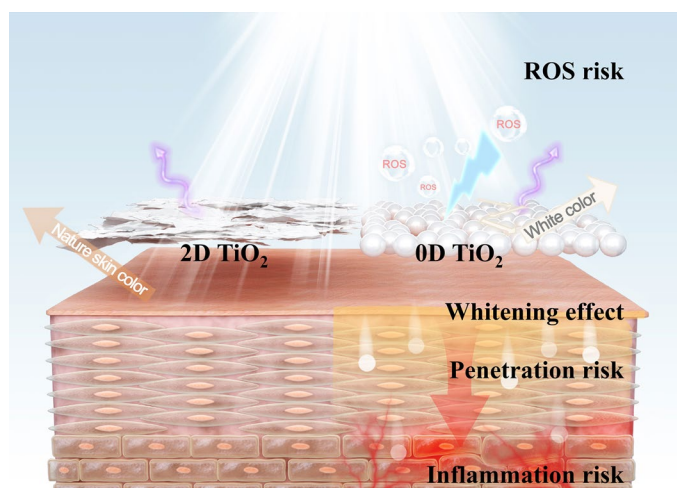
© The Author(s) 2025

Ruoning Yang¹, Jiefu Chen¹, Xiang Li¹, Yaxin Zhang¹, Baofu Ding^{2,3} ✉, Yujiangsheng Xu⁴, Shaoqiang Luo⁴, Shaohua Ma⁵, Xingang Ren⁶, Gang Liu⁷, Ling Qiu¹ ✉, Hui-Ming Cheng^{2,3,6} ✉

HIGHLIGHTS

- Two-dimensional (2D) TiO₂ was developed with > 99% visible light transmittance for non-whitening UV protection, outperforming conventional 0D TiO₂ in aesthetics while matching UV-blocking efficacy.
- 2D TiO₂ achieves ultralow skin penetration and 90% reduced reactive oxygen species generation versus 0D TiO₂, eliminating photocatalytic toxicity and DNA damage risks.
- 2D TiO₂ enabled tunable UVA/UVB coverage via metal doping without compromising visible light transmittance, ensuring Scientific Committee on Consumer Safety compliance and biocompatibility.
- We integrated high UV protection, natural appearance, and photoinertness into a single material, redefining aesthetic-safe sunscreen design through 2D structural innovation.

ABSTRACT Titanium dioxide (TiO₂) has been an important protective ingredient in mineral-based sunscreens since the 1990s. However, traditional TiO₂ nanoparticle formulations have seen little improvement over the past decades and continue to face persistent challenges related to light transmission, biosafety, and visual appearance. Here, we report the discovery of two-dimensional (2D) TiO₂, characterized by a micro-sized lateral dimension (~1.6 μm) and atomic-scale thickness, which fundamentally resolves these long-standing issues. The 2D structure enables exceptional light management, achieving 80% visible light transparency—rendering it nearly invisible on the skin—while maintaining UV-blocking performance comparable to unmodified rutile TiO₂ nanoparticles. Its larger lateral size results in a two-orders-of-magnitude reduction in skin penetration (0.96 w/w%), significantly enhancing biosafety. Moreover, the unique layered architecture inherently suppresses the generation of reactive oxygen species (ROS) under sunlight exposure, reducing the ROS generation rate by 50-fold compared to traditional TiO₂ nanoparticles. Through precise metal element modulation, we further developed the first customizable sunscreen material capable of tuning UV protection ranges and automatically matching diverse skin tones. The 2D TiO₂ offers a potentially transformative approach to modern sunscreen formulation, combining superior UV protection, enhanced safety and a natural appearance.



KEYWORDS Two-dimensional; Titanium dioxide; Sunscreen; Biosafety

Ruoning Yang, Jiefu Chen, and Xiang Li have contributed equally to this work.

✉ Baofu Ding, bf.ding@siat.ac.cn; Ling Qiu, ling.qiu@sz.tsinghua.edu.cn; Hui-Ming Cheng, cheng@imr.ac.cn

¹ Shenzhen Geim Graphene Center (SGC), Tsinghua Shenzhen International Graduate School (SIGS), Tsinghua University, Shenzhen 518055, People's Republic of China

Published online: 17 June 2025



SHANGHAI JIAO TONG UNIVERSITY PRESS

Springer

1 Introduction

Skin cancer is a significant threat to human health. As reported in a World Health Organization report in 2020, there are over 1.5 million annual diagnosed cases of skin cancer worldwide, with approximately 8% of patients experiencing a fatal outcome [1]. Excessive exposure to ultraviolet (UV) radiation stands as the foremost cause, contributed to more than 90% of all skin cancer cases [2]. Human efforts to shield against UV radiation date back to ancient times. For instance, ancient Egyptians used natural jasmine oil and rice bran to shield their skin from UV damage [3]. With advances in optics and physiology during the twentieth century, systematic investigations on the effects of UV exposure on human skin were started, leading to rapid progress in the use of active ingredients for UV blocking. One of the significant milestones occurred in 1928 with the introduction of sunscreen containing salicylates and cinnamates as effective components [4]. Until 1969, avobenzone, capable of shielding against ultraviolet radiation A (UVA) in the 320–400 spectral range, was developed [5]. To date, the US Food and Drug Administration and European Commission certified sunscreens use mostly organic compounds, which are considered indispensable [6]. However, these organic UV-blocking additives are prone to degradation and loss of efficacy during photoactivation [7]. For instance, avobenzone can lose 36% of its absorption capacity after one hour of sunlight exposure [8]. Moreover, some organic additives can either penetrate the skin or cause potential skin sensitization in clinical settings [9–11].

Nowadays, inorganic titanium dioxide (TiO_2) was gradually proposed to replace organic additives in sunscreen formulations because of its outstanding UV stability and efficient UV shielding ability [12, 13]. This significantly prolonged the UV protection time and facilitated the rise of physical sunscreen ingredients [14, 15]. Consequently,

inorganic based sunscreens have gained significant market share in recent years [16]. TiO_2 primarily exists in two crystalline phases: rutile and anatase. The anatase phase exhibits stronger phototoxicity due to its significantly distorted octahedra and is commonly utilized as a photocatalytic material [17–21], whereas the rutile phase, with higher symmetry, demonstrates reduced phototoxicity. In accordance with the Scientific Committee on Consumer Safety guidelines [22], current physical sunscreens predominantly utilize rutile-phase TiO_2 particles in the nanometer range (> 30 nm). Current physical sunscreens mostly use spherical TiO_2 particles with sizes in a nanometer range [23]. Although zero-dimensional (0D) TiO_2 can absorb most of UV radiation, it also scatters a large portion of visible light due to its agglomeration, resulting in an aesthetically undesirable white cast on the skin [24, 25]. At the same time, due to the existence of a typical gap of about 300 nm between the flattened cells of stratum corneum, there is a continuously increasing concern regarding the potential penetration of 0D TiO_2 into the human body, as most of commercially added 0D TiO_2 has an average diameter of ~ 100 nm [26]. Pathological studies have indicated that the presence of untreated nanoscale TiO_2 in a biological system can disrupt membrane structures [27], leading to severe issues such as DNA damage [28–30]. Moreover, nanoscale TiO_2 particles still demonstrate unavoidable phototoxic effect, in which their photocatalytic effect can produce reactive oxygen species (ROS), leading to skin damage, even though treated by ion doping, coating, and adding antioxidants [31, 32]. Therefore, achieving a balance between a high UV-blocking efficiency, low phototoxicity and skin penetration while maintaining a natural skin appearance poses a critical challenge for the development of such sunscreens or skincare products that prioritize both aesthetics and health.

Here, we find that two-dimensional (2D) TiO_2 can effectively block UV radiation while having a remarkably high

² Shenzhen Key Lab of Energy Materials for Carbon Neutrality, Shenzhen Institute of Advanced Technology, Chinese Academy of Sciences, 1068 Xueyuan Road, Shenzhen 518055, People's Republic of China

³ Faculty of Materials Science and Energy Engineering, Shenzhen University of Advanced Technology, 291 Louming Road, Shenzhen 518107, People's Republic of China

⁴ Hipapa Xihe Laboratory, Run Science Park, 18 Shenzhou Road, Huangpu, Guangzhou 510663, People's Republic of China

⁵ Shenzhen Key Laboratory of Gene and Antibody Therapy, State Key Laboratory of Chemical Oncogenomics, Shenzhen International Graduate School (SIGS), Tsinghua University, Shenzhen 518055, People's Republic of China

⁶ Information Materials and Intelligent Sensing Laboratory of Anhui Province, Anhui University, Hefei 230601, People's Republic of China

⁷ Shenyang National Laboratory for Materials Science, Institute of Metal Research, Chinese Academy of Sciences, 72 Wenhua Road, Shenyang 110016, People's Republic of China

visible light transmittance, extremely low skin permeability and negligible phototoxicity (Fig. 1). In addition, the introduction of a new parameter, the Natural Appearance Factor (NAF), is discussed and applied to the 2D TiO₂ material. NAF is a measure of how a sunscreen looks on different skin types. At the standard concentration in sunscreen products, 2D TiO₂ has an ideal NAF value of 0.99, approaching the maximum value of 1.0, and effectively solves the problem of the white cast from conventional 0D TiO₂. It also has both negligible phototoxicity and skin penetration, suppressing its influence on skin damage and potential health risks in vivo. More importantly, 2D TiO₂ can also support the design of spectral coverage by doping biologically safe metals, such as iron, enabling a balanced comprehensive performance of a standard UV-blocking ratio, natural skin appearance, ultralow skin permeance, and negligible phototoxicity.

2 Results and Discussion

2.1 Optical Characteristics of 2D TiO₂ as a UV Filter

2D TiO₂ was produced by using liquid-phase ionic intercalation and exfoliation of layer-type titanate

$K_{0.8}Li_{0.27}Ti_{1.73}O_4$, and in particular, a dialysis method was used to ensure the safety of the final material to the skin (see details in Method and Fig. S1) [33–35]. The 2D TiO₂ has an average lateral size of 1.6 μm and a thickness of 1.2 nm (Fig. S2), and could be well-dispersed in water. For comparison, 0D TiO₂ with an average diameter of ~100 nm that is commonly used in the fine chemical industry and commercial sunscreen products was selected (Figs. S3 and S4). As illustrated in Fig. 2A, 2D TiO₂ has full ultraviolet radiation B (UVB) blocking capability in the 280–320 nm spectral range, while maintaining a transmittance of > 80% across the entire visible spectrum. In contrast, 0D TiO₂ has a much lower overall visible light transmittance than 2D TiO₂ due to their strong scattering. A 2D TiO₂ dispersion of the same concentration is more transparent than that of a 0D TiO₂ dispersion (Fig. S5). SPF is a widely accepted parameter for evaluating UV protection ability [36, 37]. Inspired by the definition of SPF, we introduce NAF, a parameter that quantitatively demonstrates the ability of a material to retain the natural appearance of a human skin (for details of its definition and calculation see discussion section S1 and Fig. S6). A NAF value close to 1 indicates a material that more accurately retains the natural

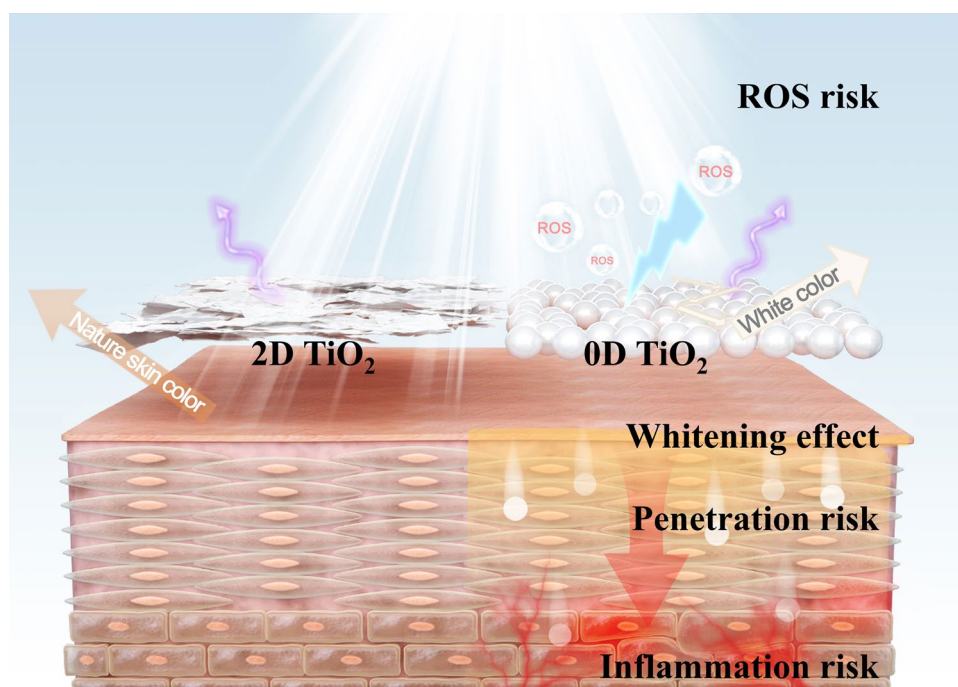


Fig. 1 Scheme of impact of 2D TiO₂ (left side) accompanied with natural skin color and no security risk, and 0D TiO₂ (right side) accompanied with whitening phenomenon, free radical production and penetration on the appearance of skin surface

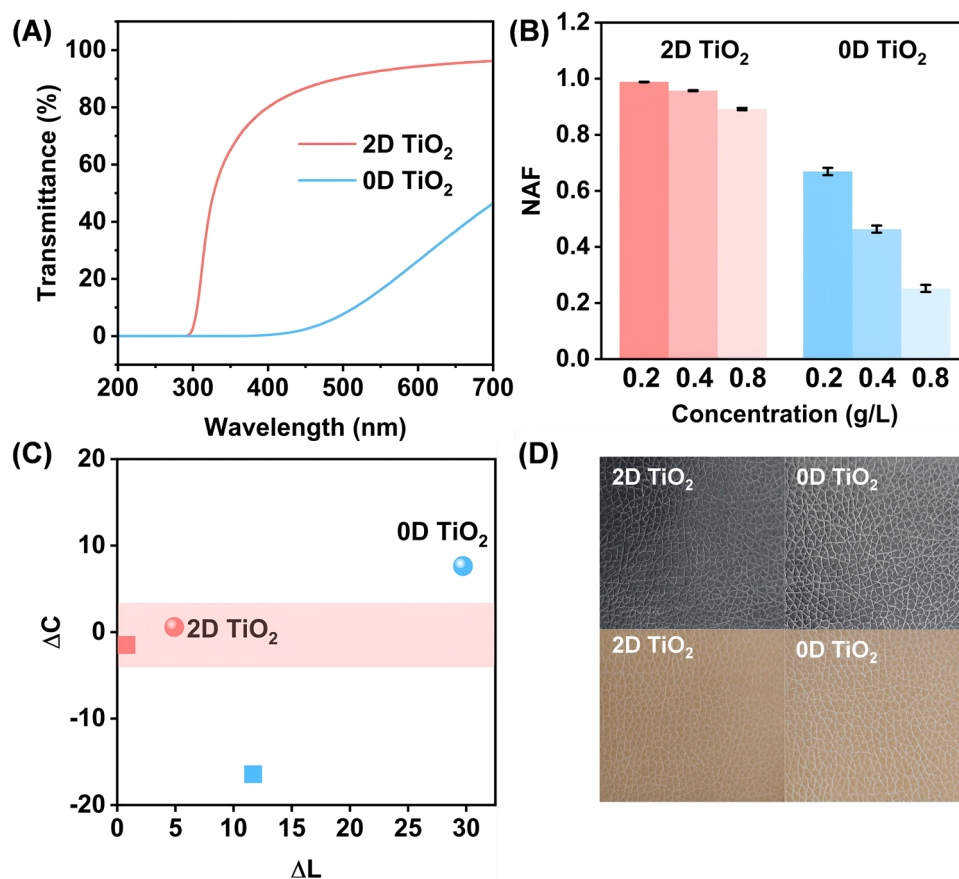


Fig. 2 Optical characterization of 2D TiO₂. **A** UV–visible transmittance spectra of a 0.8 g L⁻¹ aqueous 2D TiO₂ solution and 0D TiO₂ solution. **B** NAF for 0.2, 0.4, and 0.8 g L⁻¹ aqueous 2D TiO₂ solutions and 0D TiO₂ solutions. **C** Changing in saturation (ΔC) and lightness (ΔL) relative to the original leather color when coating with emulsions with a 4 w/w% solid content on synthetic leather, where the spherical shape represents the application on black leather, while the square shape represents the application on khaki leather. Smaller absolute values of ΔC and ΔL indicate less color alteration after emulsion coating, consistent with the requirement of a natural appearance. **D** Photographs of top views of emulsions with 4 w/w% solid content coated on synthetic leather, corresponding to **C**

appearance of the skin. The NAF values for 0.2, 0.4, and 0.8 g L⁻¹ aqueous 2D TiO₂ and 0D TiO₂ solutions were calculated accordingly (Fig. 2B). For a given concentration, the NAF of 2D TiO₂ is commonly much higher than that of 0D TiO₂. As the concentration increases from 0.2 to 0.8 g L⁻¹, the NAF for the aqueous 2D TiO₂ solution decreases slightly from 0.99 to 0.89. In contrast, the NAF for the aqueous 0D TiO₂ dispersion drops sharply from 0.67 to 0.25. This quantitatively reflects the more intense whitening with an increasing concentration of 0D TiO₂, while 2D TiO₂ maintain high visible light transmittance. To visually examine the difference in appearance, we prepared two emulsions containing the same concentrations of 2D and 0D TiO₂ and then applied them to synthetic black and khaki leathers, which were used to simulate different

human skin tones. By testing the difference of lightness (ΔL) and saturation (ΔC) of the leathers after coating with the TiO₂ emulsions, it was clearly seen that the leather coated by 2D TiO₂ had lower ΔL and ΔC values compared with the one covered with 0D TiO₂ (Fig. 2C). And a clear visual difference could be observed in leathers coated with the two TiO₂ concentrations, as shown in Fig. 2D.

To study the mechanism for the high visible light transmittance of 2D TiO₂, samples with different thicknesses were prepared by controlling the treatment time of tetrabutylammonium hydroxide. Figure 3A and B shows that a shorter treatment time results in a thicker 2D TiO₂. The optical characteristics of 2D TiO₂ and 0D TiO₂ at the same concentration were determined using UV–visible spectroscopy, and it was found that reflection from

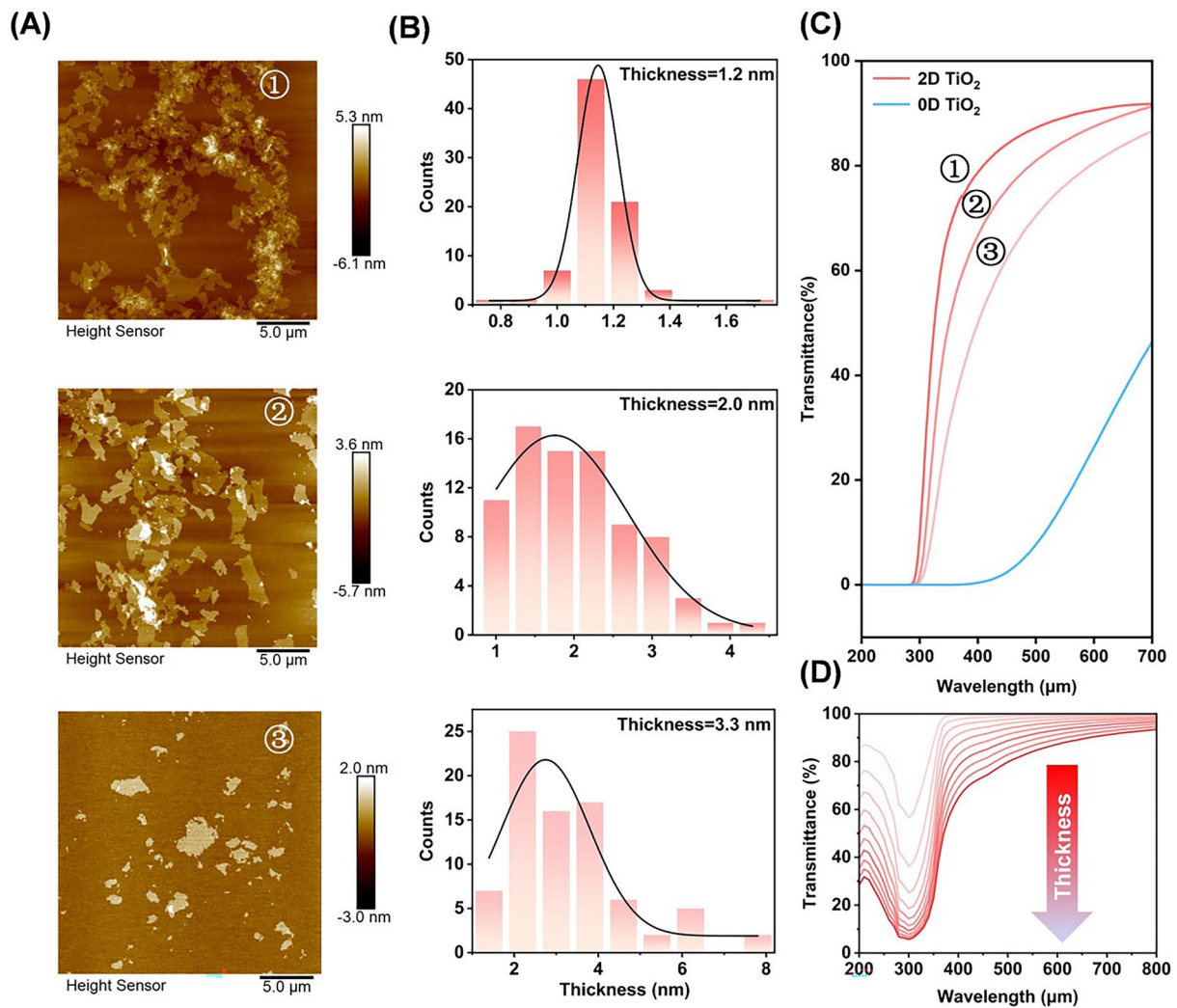


Fig. 3 Mechanisms of the high NAF of 2D TiO₂. **A** AFM image and **B** thickness distribution of 2D TiO₂ under different preparation conditions, where ①, ②, and ③ are samples with different thicknesses. **C** UV–visible spectra of 2D TiO₂ with different thicknesses and of 0D TiO₂. **D** Simulation of the optical transmittance of 2D TiO₂ with thicknesses of 1 to 10 nm

2D TiO₂ gradually increases with increasing thickness and approaches that of 0D TiO₂ (Fig. 3C). To understand the reason why the 2D TiO₂ possess such high visible light transmittance, we simulated the light transmittance of 2D TiO₂ at different thicknesses (see details in discussion section S2). As their thickness increases from 1 to 10 nm, the 2D TiO₂ has a pronounced loss of transmittance in the range 200–400 nm (Fig. 3D), which is centered at 300 nm, the intrinsic absorption peak of TiO₂ (Fig. S7). No significant absorption was observed in the visible light spectrum for the different thicknesses, despite a decrease in transmittance, so the loss is attributed to the increased reflectance

of the sheets as their thickness grows, which substantially reduces overall transmittance. In other words, the ultra-thin thickness of 2D TiO₂ suppresses the reflection and scattering of visible light, while maintaining UV-absorption capability.

2.2 Low Phototoxicity of 2D TiO₂

Another health concern of the TiO₂ additive is phototoxicity. Upon absorbing UV light, TiO₂ generates excitons that interact with oxygen or water in the environment and

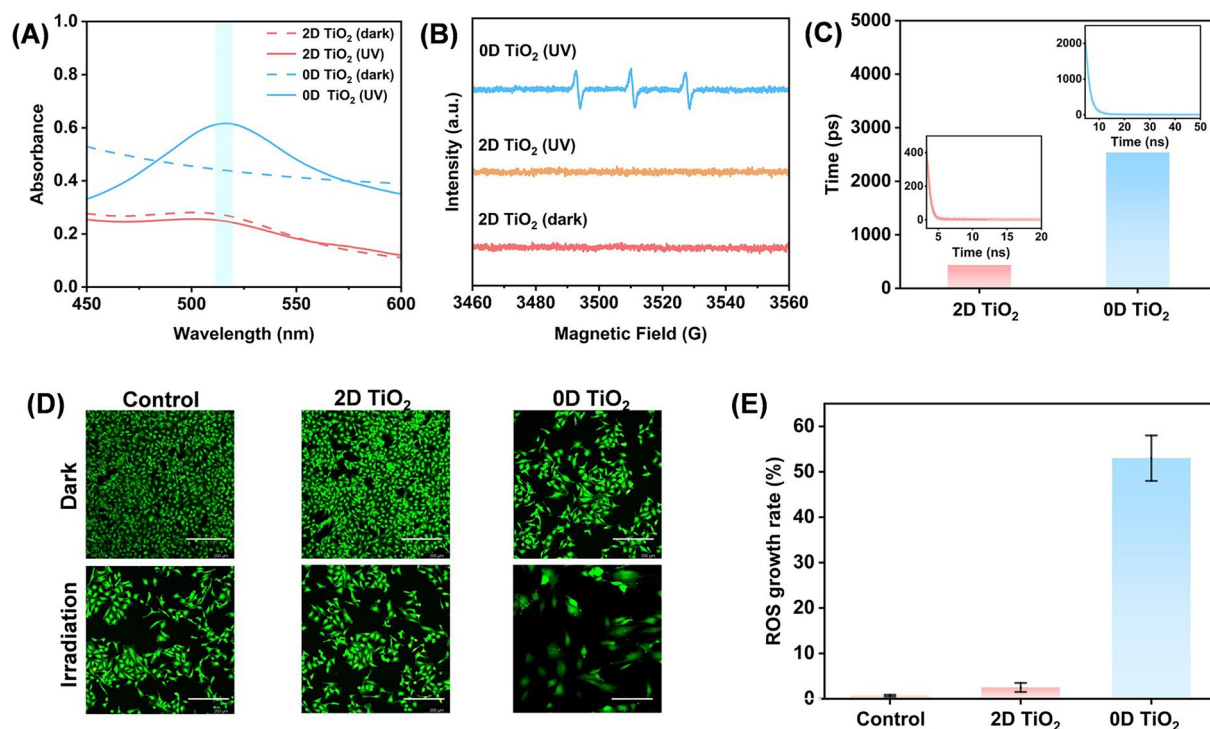


Fig. 4 Phototoxicity of 2D TiO₂. **A** Radical scavenging test of TiO₂ for DPPH, showing the DPPH absorption peaks before and after UV irradiation. With equal initial concentrations of DPPH, differences in the absorption peaks under dark conditions possibly arise from the adsorption of DPPH by TiO₂. **B** EPR analysis of reactive oxygen species generated by TiO₂ under UV irradiation. **C** Lifetime of transient photo-generated excitons in 2D TiO₂ and 0D TiO₂ from photoluminescence spectra. The insets show the lifetime of excitons as a function of intensity. **D** Fluorescence images of HSF cells before and after UV irradiation. Scale bar 200 μm. **E** Effect of different types of TiO₂ on the ROS growth rate of HSF under UV irradiation

consequently produce ROS. These radicals may subsequently cause phototoxic reactions on the skin to accelerate skin aging [38]. To quantitatively examine the phototoxicity of 2D TiO₂, we conducted tests according to the Safety and Technical Standards for Cosmetics (2015). First, we used 1,1-diphenyl-2-picrylhydrazyl (DPPH) to detect free radicals generated by TiO₂ under UV irradiation (Fig. 4A). Apart from the radical scavenging caused by the UV irradiation itself, the scavenging rate by 2D TiO₂ (5%) was five-times less than that by 0D TiO₂ (25%), and no detectable ROS was observed in the dispersion of 2D TiO₂ by electron paramagnetic resonance (EPR) (Fig. 4B and Table S1).

It is important to note that the result is contrary to intuition, because the large specific surface area of 2D materials may provide more exposed active reaction sites and result in higher photocatalytic efficiency. Actually, the photocatalytic efficiency of TiO₂ is determined by the interplay

between the recombination and capture of photo-generated carriers and the interfacial charge transfer of captured carriers [39, 40]. For charge separation, holes in the valence band and electrons in the conduction band migrate to the surface of 2D TiO₂, where they participate in the redox reactions, driving various photocatalytic processes [41]. In this regard, although 2D TiO₂ has a larger specific surface area, it also provides more recombination centers or sites for photo-generated electrons and holes [42]. This phenomenon effectively decreases the number of photo-generated free carriers, as evidenced by the much-shortened lifetime of the photo-generated excitons in 2D TiO₂ (Fig. 4C). The phototoxicity of TiO₂ was also assessed by cellular experiments. In co-culture with HeLa cells (Fig. S8) and human skin fibroblasts (HSF) (Fig. 4D), the cytotoxicity of both 2D and 0D TiO₂ is low under dark conditions. When applying UV irradiation, the ROS produced by 0D TiO₂ significantly

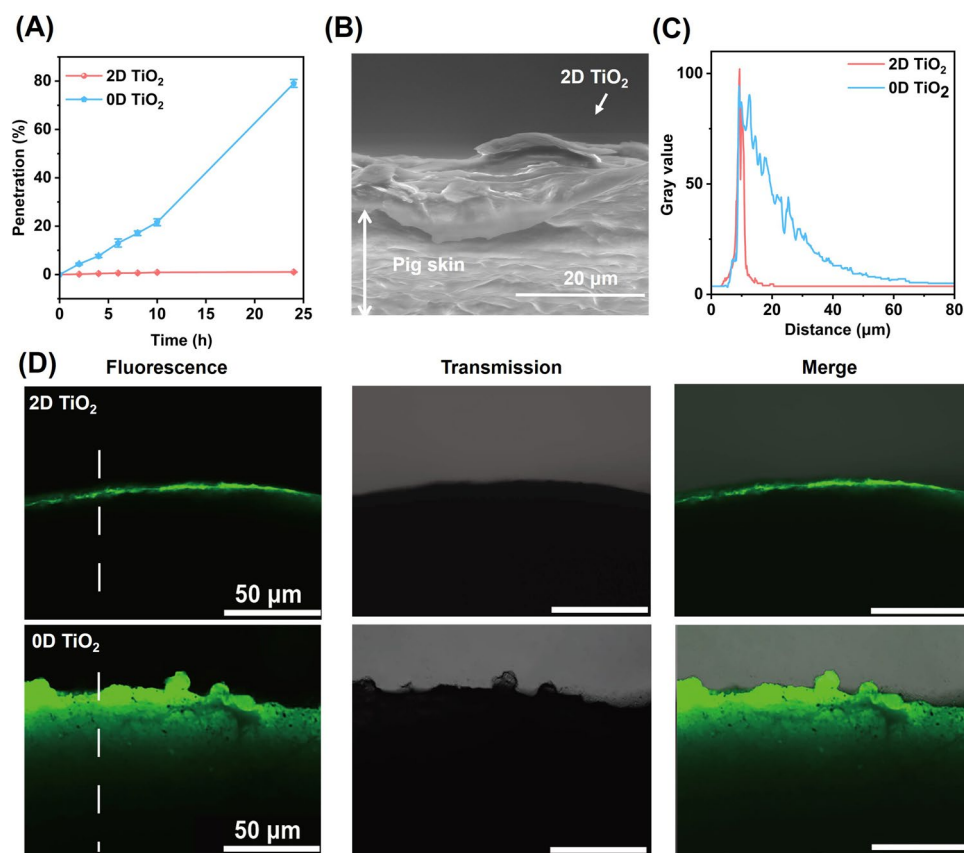


Fig. 5 Skin penetration of 2D TiO₂. **A** Curves depicting the mass percent of 2D and 0D TiO₂ penetrating into a receiving pool over time in the Franz diffusion cell test, with testing time ranging from 2 to 24 h. **B** Environmental SEM image of the cross section of pig skin coated by the emulsion containing 2D TiO₂. **C** Gray value as a function of distance, representing the fluorescence intensity and distance mapping of the dashed region corresponding to the fluorescence microscopy image in **D**. **D** Fluorescence images of labeled 2D TiO₂ (upper ones) and 0D TiO₂ (lower ones) on pig skin after 4 h of application

lower the cell survival rate, while 2D TiO₂ has a negligible influence, indicating its low phototoxicity (Fig. 4E).

2.3 Low Skin Penetration of 2D TiO₂

We investigated the skin permeability of 2D TiO₂ using a Franz diffusion cell method, an established in vitro technique for assessing permeability [43] with phosphate buffered saline used to simulate the human body environment, and 3 M synthetic skin used as a skin model (Fig. S9). Samples were taken from a receiving pool, and the permeation rate was measured every two hours. After ten hours of permeation, we observed that the permeation rate of 2D TiO₂ was approximately 0.91 w/w%, while that of 0D TiO₂ was about 21.8 w/w% (Fig. 5A). During the subsequent 14 h (from

10 to 24 h), the permeation rate of 2D TiO₂ remained stable at 0.96 w/w%, whereas that of 0D TiO₂ increased up to 77.2 w/w%. These results suggest that the permeation of 2D TiO₂ gradually decreased over time, which indicates a self-inhibitory effect of 2D TiO₂ for preventing the diffusion of TiO₂ into the skin.

The low permeability of 2D TiO₂ was determined by its morphology. The sheet-like characteristic results in a structure resembling the stratum corneum when 2D TiO₂ emulsion adhered to the surface of pig skin (Fig. 5B). However, due to a lateral size smaller than the gaps in the stratum corneum, 0D TiO₂ can easily penetrate into deep layers of the skin, posing a potential risk of hemotoxicity and genotoxicity.

We also investigated the permeation of 2D TiO₂ using a pig skin model, due to its close resemblance to human skin.

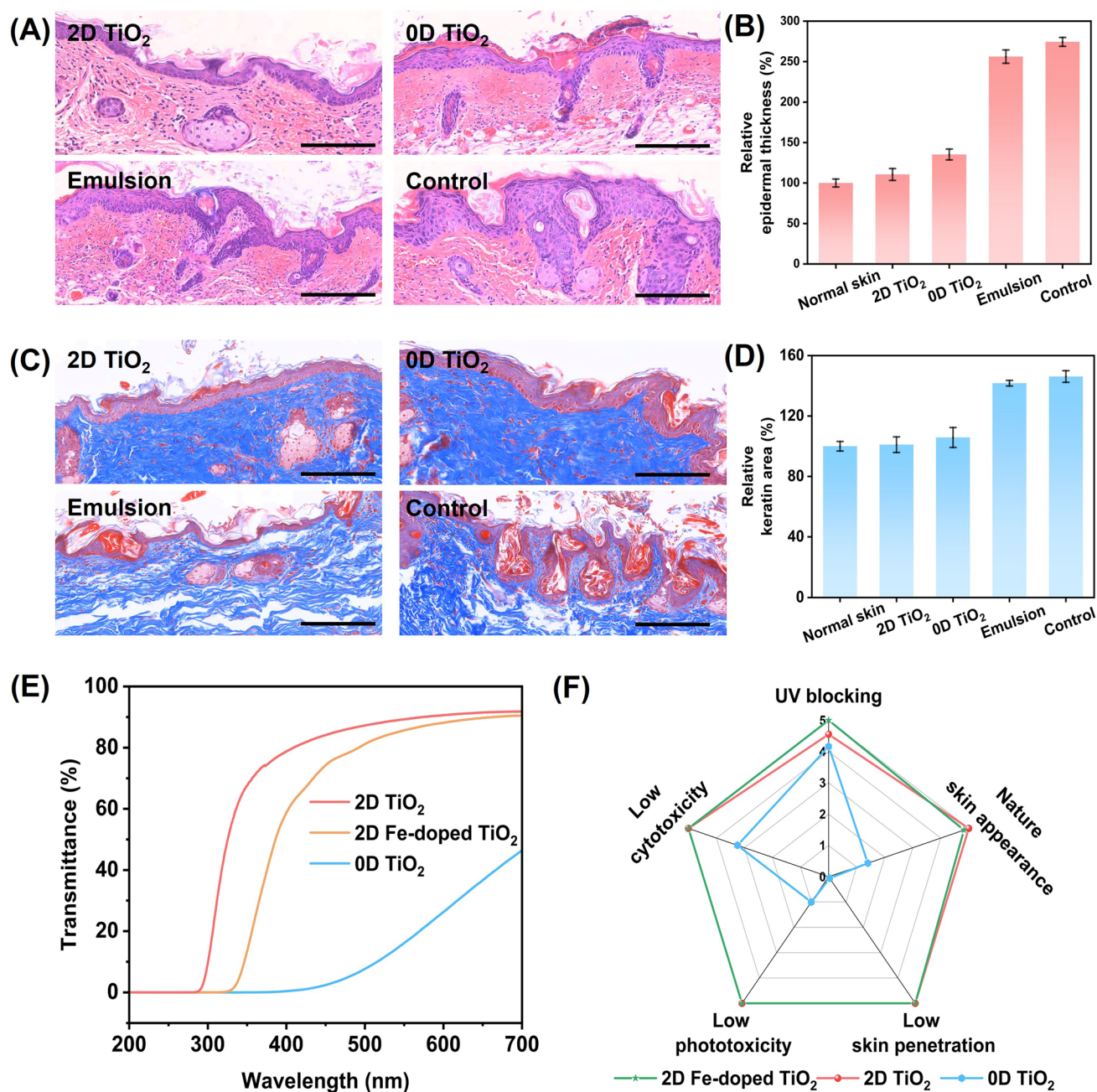


Fig. 6 A conceptual prototype of sunscreens with 2D TiO₂ and doped 2D TiO₂. **A** and **B** Statistics on epidermal thickening in mouse skin and histological sections stained with H&E of sunscreens with 2D TiO₂ and 0D TiO₂, pure emulsion, and unprotected controls. **C** and **D** Statistics of the keratin increase in mouse skin and sections with Masson's trichrome staining of the aforementioned sunscreens. All scale bars are 100 μ m. **E** Transmittance spectra of 2D TiO₂ doped with iron. **F** Radar graph of integrated performance of three types of TiO₂

Using a fluorescence labeling method, equal amounts of 2D and 0D TiO₂ were applied to the surface of pig skin, and the permeation was observed by a fluorescence microscope. The dotted section in the fluorescence image was selected to generate the relationship between fluorescence intensity and penetration depth (Fig. 5C). Figure 5D illustrates the

penetration depth of TiO₂ on the pig skin surface 4 h after coating. It can be clearly seen that the 2D TiO₂ stayed more on the pig skin surface, whereas nanoparticles penetrated it to a depth of > 20 μ m.

2.4 A Conceptual Prototype for Sunscreens

To simulate the actual use of sunscreen agents, we developed a minimalist sunscreen formula by incorporating 4 w/w% of either 2D or 0D TiO₂ into an emulsion suitable for direct application to the skin (Fig. S10). It is known that the harmful UV spectrum affecting the skin covers UVA and UVB [44]. However, the protection provided by TiO₂ is primarily in the UVB range due to its intrinsic electronic structure. To enhance protection, we compounded a certain amount of organic sunscreen agents to broaden the absorption wavelength to the UVA spectrum. We then investigated the effectiveness of these emulsions in protecting against UV-induced skin damage.

UV exposure is known to cause epidermal thickening and increase keratin content in the skin. Using the aforementioned emulsions as protective materials, we examined nude mouse skin tissue after UV irradiation hematoxylin–eosin (H&E) and Masson's trichrome staining. The UV treatment lasted for 3 days, with 15 min of exposure per day. Controls included the emulsion base without UV filters and an unprotected control.

As shown in Fig. 6A, the epidermis of mice protected by other emulsions was twice the thickness of those protected by the emulsion with 2D TiO₂. Quantitative analysis (Fig. 6B) shows that the epidermis of mice protected with 2D TiO₂ remains at the same level as normal skin, while that of mice protected with 0D TiO₂ was 120% thicker than normal skin, those of mice protected with the emulsion and unprotected mice were 256% and 275% thicker than normal skin, respectively. As shown in Figs. 6C and D, in the skin tissues of mice without the protection of TiO₂, there were broken keratin fibers and more pores, with a significant increase in keratin content. Although the increase in keratin content in the skin tissue of mice protected with 0D TiO₂ was not significant, severe fiber breakage and many pores were observed, affecting the original structure of the skin, likely related to the penetration of nanoparticles. In contrast, no significant increase in keratin was observed in the skin tissue of mice protected with 2D TiO₂, indicating its effective prevention of skin keratinization.

We also compared the white-cast effect of the two proof-of-concept products. After patch testing approval (See details in data S1 and data S2), the emulsions were applied to the back of the human hand. The skin's natural appearance in the emulsion without TiO₂ was clearly identified. While

areas coated with 0D TiO₂ showed whitening, and those coated with 2D TiO₂, with a previously calculated NAF of 0.89 (Fig. S11), had an appearance almost identical to the original skin. Another distinctive advantage of 2D TiO₂ lies in its tailorable optical properties by metal doping. The incorporation of appropriate elements can broaden or red-shift the absorption peak of TiO₂, thereby compensating for the insufficient absorption of pure TiO₂ in the UVA range. We therefore tried to introduce iron into the TiO₂ lattice and obtained iron-doped 2D TiO₂ (synthesis process and morphology seen in Figs. S12–S14). The XPS spectra in Fig. S15 indicate that iron is doped in the 2D TiO₂, making it a UV filter with a broader spectrum (Fig. 6E), which possibly supports the full use of inorganic UV-blocking additive in future sunscreens. Because of the excellent performance of the 2D material (Fig. 6F), the 2D Fe-doped TiO₂ and its formulated emulsions maintain a high visible light transmittance (Figs. S16 and S17) and low phototoxicity (Fig. S18). In addition, compared with commercial sunscreens, the sunscreen cream with 4 w/w% 2D Fe-doped TiO₂ has a much higher UV protection efficiency in vivo (Figs. S19 and S20).

3 Conclusions

We have systematically compared the optical properties, photochemical reaction activity and penetration of 2D TiO₂ and 0D TiO₂. 2D TiO₂ UV filters demonstrated many unique advantages such as desired UV damage-prevention, high visible light transmittance, extremely low phototoxicity, and minimal skin permeability. A proof-of-concept sunscreen based on a 2D TiO₂ additive was produced with these advantages. Tailoring the UV-blocking properties of 2D TiO₂ proved to be possible by introducing a selective dopant (Fe) to the matrix of 2D TiO₂, while maintaining both an excellent natural skin appearance and biosafety. This work introduces a new class of UV filters that overcome the limitations of traditional sunscreen agents, such as high toxicity and whitening effects, thereby paving the way for the development of next-generation sunscreens.

Acknowledgements This work was supported by the National Key Research and Development Project (No. 2019YFA0705403), the National Natural Science Foundation of China (No. T2293693, 52273311), the Guangdong Basic and Applied Basic Research Foundation (No. 2020B0301030002), and the Shenzhen Basic Research Project (Nos. WDZC20200824091903001,

JSGG20220831105402004, JCYJ20220818100806014). Shenzhen Major Science and Technology Projects (Nos. KCXFZ20240903094013018, KCXFZ20240903094203005). We thank P. A. Throver for carefully reviewing and revising the manuscript. Y.X. and S.L. for providing in-depth help on examining the application of 2D TiO₂ in sunscreen.

Author Contributions H.M.C. and L.Q. conceived the idea, and L.Q., B.F.D., and H.M.C. supervised the project. R.N.Y., J.F.C., and X.L. conducted experiments and data analysis. The theoretical simulation was done by G.X.R., and the industrialization verification was carried out by Y.X.Z., Y.J.S.X., and S.Q.L. Besides, S.H.M. provided professional advice on the biological experiments. All authors have reviewed, discussed, and commented on the results, and L.Q., B.F.D. H.M.C. R.N.Y., and X. L. wrote the paper with input from all authors.

Declarations

Conflict of interests The authors declare no conflict of interest. They have no known competing financial interests or personal relationships that could have appeared to influence the work reported in this paper.

Open Access This article is licensed under a Creative Commons Attribution 4.0 International License, which permits use, sharing, adaptation, distribution and reproduction in any medium or format, as long as you give appropriate credit to the original author(s) and the source, provide a link to the Creative Commons licence, and indicate if changes were made. The images or other third party material in this article are included in the article's Creative Commons licence, unless indicated otherwise in a credit line to the material. If material is not included in the article's Creative Commons licence and your intended use is not permitted by statutory regulation or exceeds the permitted use, you will need to obtain permission directly from the copyright holder. To view a copy of this licence, visit <http://creativecommons.org/licenses/by/4.0/>.

Supplementary Information The online version contains supplementary material available at <https://doi.org/10.1007/s40820-025-01805-1>.

References

1. H. Sung, J. Ferlay, R.L. Siegel, M. Laversanne, I. Soerjomataram et al., Global cancer statistics 2020: GLOBOCAN estimates of incidence and mortality worldwide for 36 cancers in 185 countries. *CA Cancer J. Clin.* **71**(3), 209–249 (2021). <https://doi.org/10.3322/caac.21660>
2. G.K. Griffin, C.A.G. Booth, K. Togami, S.S. Chung, D. Szozi et al., Ultraviolet radiation shapes dendritic cell leukaemia transformation in the skin. *Nature* **618**(7966), 834–841 (2023). <https://doi.org/10.1038/s41586-023-06156-8>
3. A.S. Aldahan, V.V. Shah, S. Mlacker, K. Nouri, The history of sunscreen. *JAMA Dermatol.* **151**(12), 1316 (2015). <https://doi.org/10.1001/jamadermatol.2015.3011>
4. Y. Ma, J. Yoo, History of sunscreen: an updated view. *J. Cosmet. Dermatol.* **20**(4), 1044–1049 (2021). <https://doi.org/10.1111/jocd.14004>
5. D.L. Giokas, A. Salvador, A. Chisvert, UV filters: from sunscreens to human body and the environment. *TrAC Trends Anal. Chem.* **26**(5), 360–374 (2007). <https://doi.org/10.1016/j.trac.2007.02.012>
6. M.N. Pantelic, N. Wong, M. Kwa, H.W. Lim, Ultraviolet filters in the United States and European union: a review of safety and implications for the future of US sunscreens. *J. Am. Acad. Dermatol.* **88**(3), 632–646 (2023). <https://doi.org/10.1016/j.jaad.2022.11.039>
7. Y. Huang, J.C. Law, T.-K. Lam, K.S. Leung, Risks of organic UV filters: a review of environmental and human health concern studies. *Sci. Total. Environ.* **755**, 142486 (2021). <https://doi.org/10.1016/j.scitotenv.2020.142486>
8. A.R. Abid, B. Marciniak, T. Pędziński, M. Shahid, Photo-stability and photo-sensitizing characterization of selected sunscreens' ingredients. *J. Photochem. Photobiol. A Chem.* **332**, 241–250 (2017). <https://doi.org/10.1016/j.jphotochem.2016.08.036>
9. J. Ao, T. Yuan, L. Gao, X. Yu, X. Zhao et al., Organic UV filters exposure induces the production of inflammatory cytokines in human macrophages. *Sci. Total. Environ.* **635**, 926–935 (2018). <https://doi.org/10.1016/j.scitotenv.2018.04.217>
10. D. Vuckovic, A.I. Tinoco, L. Ling, C. Renicke, J.R. Pringle et al., Conversion of oxybenzone sunscreen to phototoxic glucoside conjugates by sea anemones and corals. *Science* **376**(6593), 644–648 (2022). <https://doi.org/10.1126/science.abn2600>
11. J. Wang, L. Pan, S. Wu, L. Lu, Y. Xu et al., Recent advances on endocrine disrupting effects of UV filters. *Int. J. Environ. Res. Public Health* **13**(8), 782 (2016). <https://doi.org/10.3390/ijerph13080782>
12. G.M. Murphy, Sunblocks: mechanisms of action. *Photoimmunol. Photomed.* **15**(1), 34–36 (1999). <https://doi.org/10.1111/j.1600-0781.1999.tb00051.x>
13. A.P. Popov, A.V. Priezzhev, J. Lademann, R. Myllyla. Presented at Proc. SPIE, Ottawa, Ontario, Canada, (December, 2004). <https://doi.org/10.1117/12.567423>
14. Y. Dong, S. Chen, S. Zhou, S. Hou, Q. Lu, Perspectives on the next generation of sunscreen: safe, broadband, and long-term photostability. *ACS Mater. Lett.* **1**(3), 336–343 (2019). <https://doi.org/10.1021/acsmaterialslett.9b00203>
15. C. Cayrol, J. Sarraute, R. Tarroux, D. Redoules, M. Charveron et al., A mineral sunscreen affords genomic protection against ultraviolet (UV) B and UVA radiation: in vitro and in situ assays. *Br. J. Dermatol.* **141**(2), 250–258 (1999). <https://doi.org/10.1046/j.1365-2133.1999.02973.x>
16. C. Chaiyabutr, T. Sukakul, T. Kumpangsin, M. Bunyavaree, N. Charoenpipatsin et al., Ultraviolet filters in sunscreens and cosmetic products: a market survey. *Contact Dermat.* **85**(1), 58–68 (2021). <https://doi.org/10.1111/cod.13777>
17. R. Ghamarpoor, A. Fallah, M. Jamshidi, Investigating the use of titanium dioxide (TiO₂) nanoparticles on the amount of protection against UV irradiation. *Sci. Rep.* **13**(1), 9793 (2023). <https://doi.org/10.1038/s41598-023-37057-5>

18. R. Ghamarpoor, A. Fallah, M. Jamshidi, A review of synthesis methods, modifications, and mechanisms of ZnO/TiO₂-based photocatalysts for photodegradation of contaminants. *ACS Omega* **9**(24), 25457–25492 (2024). <https://doi.org/10.1021/acsomega.3c08717>
19. R. Ghamarpoor, M. Jamshidi, A. Fallah, M. Neshastehgar, Designing a smart acrylic photocatalyst coating loaded with N/C-doped TiO₂@SiO₂ core-shell by bio-based Tarem-rice husk waste for organic pollutant degradation. *Alex. Eng. J.* **115**, 131–146 (2025). <https://doi.org/10.1016/j.aej.2024.12.023>
20. Y. Li, L. Ding, S. Yin, Z. Liang, Y. Xue et al., Photocatalytic H₂ evolution on TiO₂ assembled with Ti₃C₂ MXene and metallic 1T-WS₂ as co-catalysts. *Nano-Micro Lett.* **12**(1), 6 (2019). <https://doi.org/10.1007/s40820-019-0339-0>
21. C. Zhang, H. Hua, J. Liu, X. Han, Q. Liu et al., Enhanced photocatalytic activity of nanoparticle-aggregated Ag-AgX(X = Cl, Br)@TiO₂ microspheres under visible light. *Nano-Micro Lett.* **9**(4), 49 (2017). <https://doi.org/10.1007/s40820-017-0150-8>
22. S.C.C.S. Qasim Chaudhry, Chaudhry, opinion of the scientific committee on consumer safety (SCCS)—revision of the opinion on the safety of the use of titanium dioxide, nano form, in cosmetic products. *Regul. Toxicol. Pharmacol.* **73**(2), 669–670 (2015). <https://doi.org/10.1016/j.yrtph.2015.09.005>
23. V.G. Bairi, J.-H. Lim, A. Fong, S.W. Linder, Size characterization of metal oxide nanoparticles in commercial sunscreen products. *J. Nanopart. Res.* **19**(7), 256 (2017). <https://doi.org/10.1007/s11051-017-3929-0>
24. X. Yan, V. Piffaut, F. Bernerd, C. Marionnet, M. Alyas et al., 54079 new tinted mineral sunscreen shades for skin of color populations. *J. Am. Acad. Dermatol.* **91**(3), AB65 (2024). <https://doi.org/10.1016/j.jaad.2024.07.268>
25. F. Wang, R. Lyu, H. Xu, R. Gong, B. Ding, Tunable colors from responsive 2D materials. *Responsive Mater.* **2**(3), e20240007 (2024). <https://doi.org/10.1002/rpm.20240007>
26. M. Mahmoudi, K. Azadmanesh, M.A. Shokrgozar, W.S. Journeay, S. Laurent, Effect of nanoparticles on the cell life cycle. *Chem. Rev.* **111**(5), 3407–3432 (2011). <https://doi.org/10.1021/cr1003166>
27. A.R. Young, J. Claveau, A.B. Rossi, Ultraviolet radiation and the skin: photobiology and sunscreen photoprotection. *J. Am. Acad. Dermatol.* **76**(3S1), S100–S109 (2017). <https://doi.org/10.1016/j.jaad.2016.09.038>
28. N. Serpone, A. Salinaro, A. Emeline. Presented at Proc. SPIE, San Jose, CA, United States (2001). <https://doi.org/10.1117/12.430765>.
29. R. Dunford, A. Salinaro, L. Cai, N. Serpone, S. Horikoshi et al., Chemical oxidation and DNA damage catalysed by inorganic sunscreen ingredients. *FEBS Lett.* **418**(1–2), 87–90 (1997). [https://doi.org/10.1016/S0014-5793\(97\)01356-2](https://doi.org/10.1016/S0014-5793(97)01356-2)
30. A.S. Barnard, One-to-one comparison of sunscreen efficacy, aesthetics and potential nanotoxicity. *Nat. Nanotechnol.* **5**(4), 271–274 (2010). <https://doi.org/10.1038/nnano.2010.25>
31. W. Zhao, W. Fu, H. Yang, C. Tian, M. Li et al., Synthesis and photocatalytic activity of Fe-doped TiO₂ supported on hollow glass microbeads. *Nano-Micro Lett.* **3**(1), 20–24 (2011). <https://doi.org/10.1007/BF03353647>
32. B. Ding, Y. Pan, Z. Zhang, T. Lan, Z. Huang et al., Largely tunable magneto-coloration of monolayer 2D materials *via* size tailoring. *ACS Nano* **15**(6), 9445–9452 (2021). <https://doi.org/10.1021/acsnano.1c02259>
33. T. Sasaki, M. Watanabe, H. Hashizume, H. Yamada, H. Nakazawa, Macromolecule-like aspects for a colloidal suspension of an exfoliated titanate. Pairwise association of nanosheets and dynamic reassembling process initiated from it. *J. Am. Chem. Soc.* **118**(35), 8329–8335 (1996). <https://doi.org/10.1021/ja960073b>
34. T. Tanaka, Y. Ebina, K. Takada, K. Kurashima, T. Sasaki, Oversized titania nanosheet crystallites derived from flux-grown layered titanate single crystals. *Chem. Mater.* **15**(18), 3564–3568 (2003). <https://doi.org/10.1021/cm034307j>
35. H.C. Wulf, I.M. Stender, J. Lock-Andersen, Sunscreens used at the beach do not protect against erythema: a new definition of SPF is proposed. *Photodermatol. Photoimmunol. Photomed.* **13**(4), 129–132 (1997). <https://doi.org/10.1111/j.1600-0781.1997.tb00215.x>
36. A. Faurschou, H.C. Wulf, The relation between Sun protection factor and amount of sunscreen applied *in vivo*. *Br. J. Dermatol.* **156**(4), 716–719 (2007). <https://doi.org/10.1111/j.1365-2133.2006.07684.x>
37. R. Lopez, J. Regier, M.B. Cole, M.I. Jordan, N. Yosef, Deep generative modeling for single-cell transcriptomics. *Nat. Methods* **15**(12), 1053–1058 (2018). <https://doi.org/10.1038/s41592-018-0229-2>
38. X. Ruan, S. Li, C. Huang, W. Zheng, X. Cui et al., Catalyzing artificial photosynthesis with TiO₂ heterostructures and hybrids: emerging trends in a classical yet contemporary photocatalyst. *Adv. Mater.* **36**(17), 2305285 (2024). <https://doi.org/10.1002/adma.202305285>
39. H. Huang, Y. Song, N. Li, D. Chen, Q. Xu et al., One-step *in situ* preparation of N-doped TiO₂@C derived from Ti₃C₂ MXene for enhanced visible-light driven photodegradation. *Appl. Catal. B Environ.* **251**, 154–161 (2019). <https://doi.org/10.1016/j.apcatb.2019.03.066>
40. Y. Ma, X. Wang, Y. Jia, X. Chen, H. Han et al., Titanium dioxide-based nanomaterials for photocatalytic fuel generations. *Chem. Rev.* **114**(19), 9987–10043 (2014). <https://doi.org/10.1021/cr500008u>
41. Y. Wu, W. Xu, W. Tang, Z. Wang, Y. Wang et al., *In-situ* annealed “M-scheme” MXene-based photocatalyst for enhanced photoelectric performance and highly selective CO₂ photoreduction. *Nano Energy* **90**, 106532 (2021). <https://doi.org/10.1016/j.nanoen.2021.106532>
42. S.-F. Ng, J.J. Rouse, F.D. Sanderson, V. Meidan, G.M. Eccleston, Validation of a static Franz diffusion cell system for *in vitro* permeation studies. *AAPS PharmSciTech* **11**(3), 1432–1441 (2010). <https://doi.org/10.1208/s12249-010-9522-9>
43. J. Cadet, T. Douki, J.-L. Ravanat, Oxidatively generated damage to cellular DNA by UVB and UVA radiation. *Photochem. Photobiol.* **91**(1), 140–155 (2015). <https://doi.org/10.1111/php.12368>
44. Y. Deng, A. Ediriwickrema, F. Yang, J. Lewis, M. Girardi et al., A sunblock based on bioadhesive nanoparticles. *Nat.*



Mater. **14**(12), 1278–1285 (2015). <https://doi.org/10.1038/nmat4422>

Publisher's Note Springer Nature remains neutral with regard to jurisdictional claims in published maps and institutional affiliations.